This final report is based on work described in full within a recent paper published in *Earth and Planetary Science Letters* https://doi.org/10.1016/j.epsl.2018.10.003

2018 SCEC Final Report

Award #17184: Testing fault geometry and interaction models using high-precision slip rates on the San Cayetano and Ventura-Pitas Point Faults

Principle Investigators: Dylan H. Rood
Earth Research Institute
University of California, Santa Barbara
drood@eri.ucsb.edu

In Collaboration With: Tom Rockwell (San Diego State University)
Duane DeVecchio (Arizona State University)
Craig Nicholson (UC Santa Barbara)
Scott Marshall (Appalachian State University)

Proposal Categories: **A. Data Gathering and Products**

SCEC Priorities: **Priorities P1.a, P3.a, and P5.b**

Disciplinary Activities: **C. Earthquake Geology**

Project Period: **February 1, 2017 – January 31, 2018**

This final report is based on work described in full within a recent paper published in *Earth and Planetary Science Letters* https://doi.org/10.1016/j.epsl.2018.10.003

SUMMARY OF MAIN RESEARCH FINDINGS

With our SCEC 2017 funding, we investigated surface evidence and displacement rates for a young, active, low-angle (~20°) reverse thrust fault in the footwall of the San Cayetano fault, the Southern San Cayetano fault (SSCF). Active faulting along the northern flank of the Santa Clara River Valley displaces young landforms, such as late Quaternary river terraces and alluvial fans. Geomorphic strain markers were examined using field mapping, high-resolution lidar topographic data, ^{10}Be surface exposure dating, and subsurface well data to provide evidence for a young, active SSCF along the northern flank of the Santa Clara River Valley.

Our field investigation focused on Orcutt Canyon where we conducted geomorphic mapping to identify a series of alluvial terraces and alluvial fans deformed by activity on the SSCF. We collected samples from this suite of surfaces to measure *in-situ*-produced cosmogenic ^{10}Be surface exposure ages using depth profiles. Ages for the surfaces we sampled range from 7.3 $^{+1.8}/_{-1.7}$ ka to 58.4 $^{+12.7}/_{9.0}$ ka. We then used our new ^{10}Be chronology to calculate displacement rates for the SSCF. Maximum slip rates for the central SSCF are 1.9 $^{+1.0}/_{-0.5}$ mm yr^{-1} between ~19–7 ka and minimum slip rates are 1.3 $^{+0.5}/_{-0.3}$ mm yr^{-1} since ~7 ka. Uplift rates for the central SSCF have not varied significantly over the last ~58 ka, with a maximum value of 1.7 $^{+0.9}/_{-0.6}$ mm yr^{-1} for the interval ~58–19 ka, and a minimum value 1.2 $^{+}/_{-}$ 0.3 mm yr^{-1} since ~7 ka. The SSCF is interpreted as a young, active structure with onset of activity at some point after ~58 ka.

Previous work suggested the SSCF acts as a rupture pathway to transfer strain from the Ventura fault to the San Cayetano fault in large magnitude (~Mw 8.0) earthquakes (Hubbard et al., 2014). However, the geometry for the SSCF presented here, with a ~20° north-dip in the subsurface, is the first interpretation of the SSCF based on geological field data. Our new interpretation is significantly different from the previously proposed model-derived geometry of Hubbard et al (2014), which dips more steeply at 45–60° and intersects the surface in the middle of the Santa Clara River Valley.

Based on our results, we suggest that the SSCF may rupture in tandem with the main San Cayetano fault. Additionally, the SSCF could potentially act as a rupture pathway between the Ventura and San Cayetano faults in large-magnitude, multi-fault earthquakes in southern California. However, given structural complexities, including significant changes in dip and varying Holocene displacement rates along strike, further work is required to examine the possible mechanism, likelihood, and frequency of potential through-going ruptures between the Ventura and San Cayetano faults.

This final report is based on work described in full within a recent paper published in *Earth and Planetary Science Letters* https://doi.org/10.1016/j.epsl.2018.10.003

TECHNICAL REPORT

Introduction

The Western Transverse Ranges (WTR) are a fold and thrust belt in southern California, U.S.A, resulting from regional transpression and 7-10 mm yr^{-1} of north-south directed crustal shortening (Marshall et al., 2013) caused by the restraining bend in the San Andreas fault (e.g. Wright, 1991). Range-front topography throughout most of the WTR is fault controlled and associated with uplift in the hangingwall of active, east-striking reverse faults (Fig. 1). In the past 4 decades, all earthquakes with magnitudes greater than M_w 6.0 in southern California occurred on such reverse faults. Some of these major structures, e.g., the Sierra Madre, Santa Susanna, Oak Ridge, San Cayetano, and Ventura-Pitas Point faults (Fig. 1), may be capable of multi-fault ruptures generating ~M_w 8 earthquakes. Consequently, many geological studies in the Los Angeles and Ventura Counties have concluded that thrust faults pose the greatest seismic hazard in southern California and accommodate most of the geodetically observed shortening across the region (Fig. 1) (e.g. Dolan et al., 2007; Dolan and Rockwell, 2001; Dolan et al., 1995; Shaw and Suppe, 1996). Yet the seismic hazard presented by many of these faults is ambiguous due to a paucity of geochronological data from the young deformed landforms, resulting in poorly defined deformation rates.

The San Cayetano fault has been identified as one of six major thrust fault systems, in addition to the San Andreas fault, that may be the source of a damaging large-magnitude (M_w 7-8) earthquake in southern California (Dolan et al., 1995). The San Cayetano fault, is often mapped as the most southerly fault along the northern flank of the Santa Clara River Valley (e.g. Rockwell 1988) (Fig. 1). However, recent fault modelling has suggested the existence of the SSCF farther south in the footwall of the San Cayetano fault (Hubbard et al., 2014). Furthermore, it has been suggested that the SSCF transfers strain between the Ventura-Pitas Point fault and the San Cayetano fault in large-magnitude (M_w 7–8) earthquakes close to major population centers in southern California (Hubbard et al., 2014). The SSCF is not included in current seismic hazard mapping for California (e.g. Jennings and Bryant, 2010), published geological maps (e.g. Dibblee Jr, 1990a), or the UCERF3 report for California (Field et al., 2015). However, the model-derived interpretation of the SSCF is included in the latest version

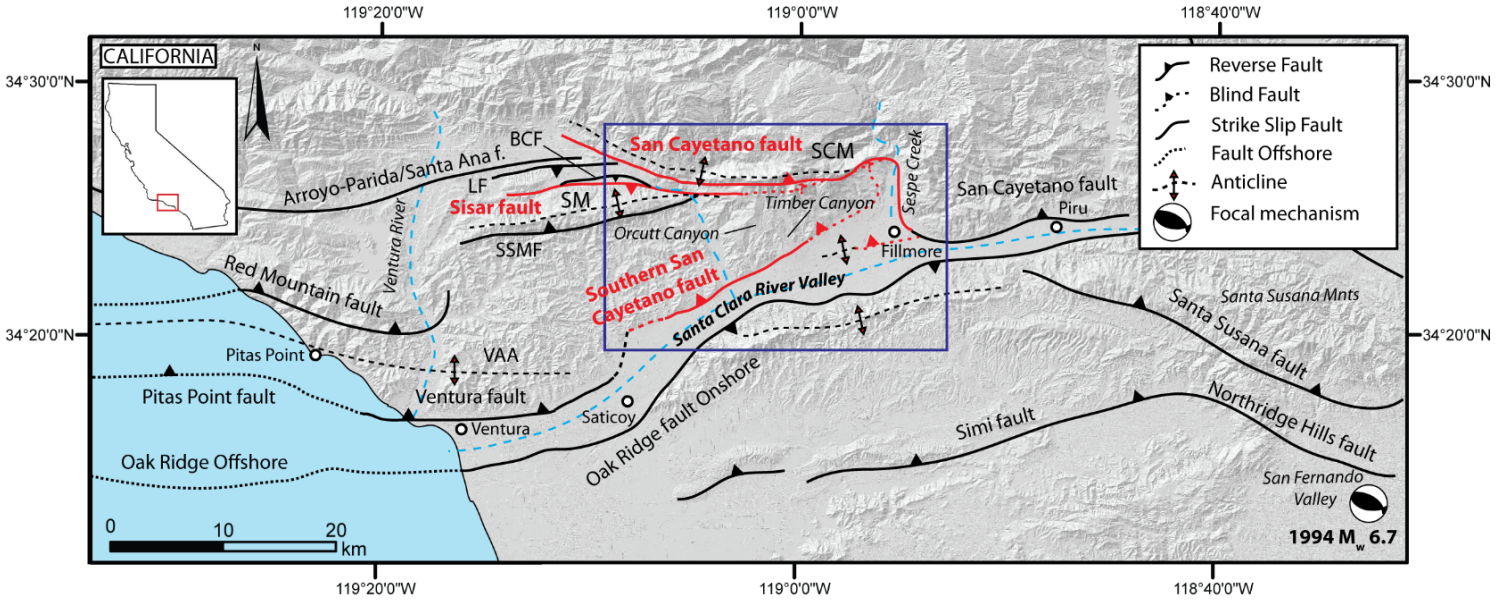

Figure 1 *Major onshore structures of the Western Transverse Ranges in the vicinity of the Southern San Cayetano fault (SSCF). The key faults discussed here are highlighted with soild red lines with other major faults denoted using solid black lines. Major regional folds are indicated by dashed black lines. The location of the earthquake focal mechanism for the 1994 M 6.7 Northridge earthquke is indicated by the beach ball. Dashed blue lines are the paths of major rivers. The blue box shows location of Figures 2 & 5. SCM = San Cayetano Mountain, SM = Sulphur Mountain, BCF = Big Canyon fault, LF = Lion fault, SSMF = South Sulphur Mountain fault.*

of the Community Fault Model for Southern California (Nicholson et al., 2015).

A series of uplifted and tilted strath terraces, fill terraces, and alluvial fan deposits are preserved along the northern flanks of the east-west trending Santa Clara River Valley, near the proposed surface trace of the SSCF (Fig. 2). We focused on Orcutt Canyon (Figs. 1 & 2) to investigate range-front faulting along the northern Santa Clara River Valley because several geomorphic observations point to active faulting in this area. Orcutt Canyon is a north-south-trending incised valley that drains into the Santa Clara River Valley. The canyon is in the central portion of the range front, and thus likely records close-to-maximum displacement if the range front were bounded by a laterally continuous fault (Fig. 2). Alluvial fans that cross the range front at the mouth of Orcutt Canyon are warped parallel to the range front creating north-side-up scarps (Fig. 3). A series of bedding plane parallel flexural slip faults such as the Rudolph, Culbertson, and Thorpe faults are well-established in the footwall of the San Cayetano fault at Orcutt Canyon (e.g. Rockwell, 1983; Rockwell, 1988) (Figs. 2, 3, & 4). Additionally, ~3 km southeast of Orcutt Canyon in the Santa Clara River Valley, a ~2 km east-west trending fold is mapped warping Quaternary alluvial fan deposits above the valley floor (Dibblee Jr, 1990b; Rockwell, 1983) (Fig. 2b).

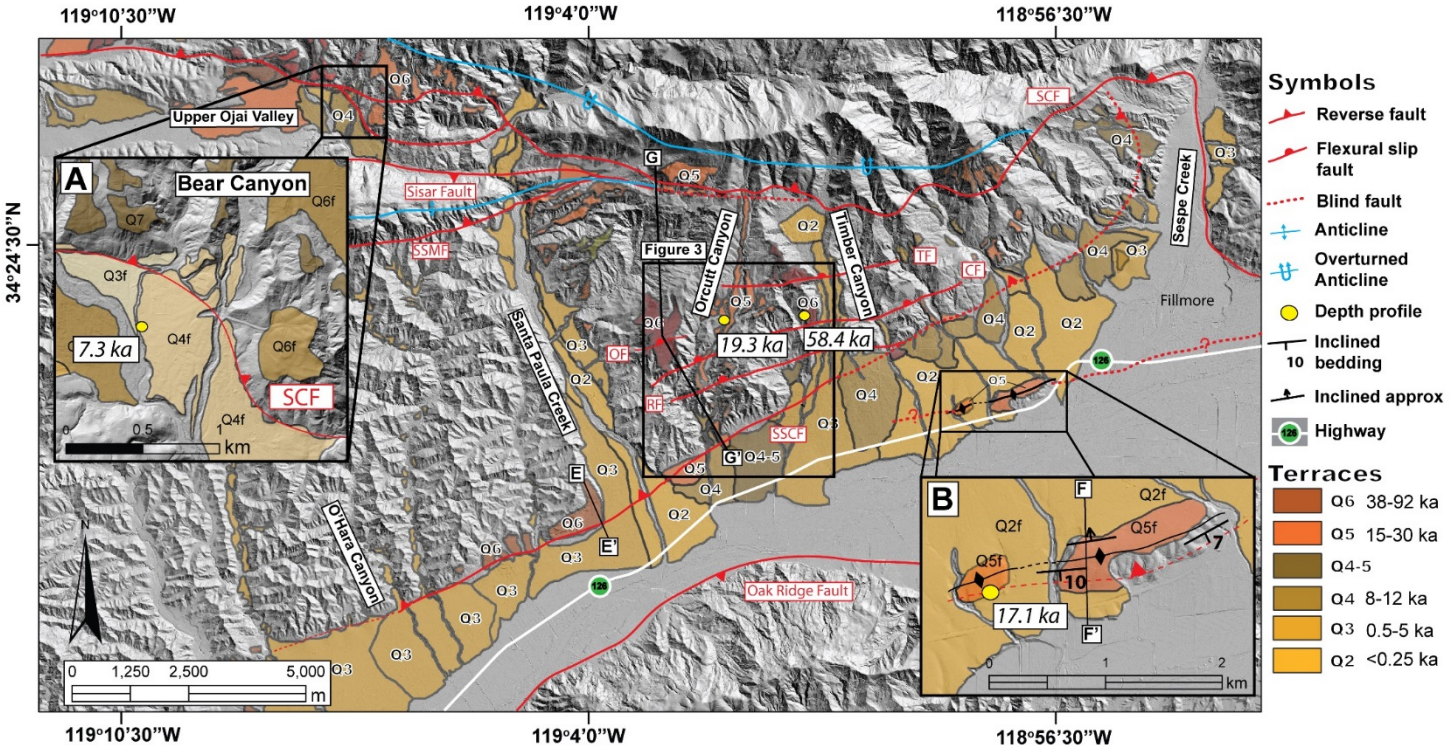

Figure 2 *Hillshade map of river terraces and alluvial fans in the proximity of the Southern San Cayetano fault (SSCF). Faults are indicated with solid red lines. Triangles and semi-circles denote fault hangingwall where triangles are reverse faults and semi-circles are flexural-slip faults. Dashed lines are blind faults. Cosmogenic depth profile locations are indicated with yellow dots. The location of Figure 3 is indicated in the black box. Line of topographic profile E-E' in Figure 4e is shown and the line of section G-G' in Figure 6 is indicated. Terrace ages are existing ages for geomorphic surfaces taken from Rockwell [1988]. (A) Map of late Quaternary alluvial fans and location of Q4 depth profile at Bear Canyon. (B) Enlarged hillshade map of the fold in the Santa Clara River Valley. Bedding readings are from Dibblee [1992]. Line of section F-F' from Figure 4f is indicated with a black line. SCF = San Cayetano fault, TF = Thorpe fault, OF = Orcutt fault, CF = Culbertson fault, RF = Rudolph fault*

A sequence of uplifted and tilted alluvial fill and strath terraces at various elevations within Orcutt Canyon have previously been mapped and numerically age dated (Rockwell, 1983; Rockwell, 1988). The existing terrace chronology for the Santa Clara River Valley and Upper Ojai Valley is based upon dendrochronology, soil development, radiocarbon, and comparative rates of faulting on the Arroyo-

Parida-Santa Ana fault (DeVecchio et al., 2012; Rockwell, 1983; Rockwell, 1988) (Fig. 1). Terraces are assigned a number that increases with increasing age, i.e. Q1 (youngest) to Q7 (oldest), and the existing terrace chronology is included in Figure 2. Terraces previously mapped at Orcutt Canyon range from Q3 (0.5-5 ka) to Q6 (38-92 ka) (Rockwell, 1983; Rockwell, 1988).

METHODOLOGY

Mapping

Geomorphic mapping was conducted at Orcutt Canyon by PI Rood with the help of one PhD student and one undergraduate student. Mapping built on existing terrace mapping of Rockwell (1983, 1988) and was supplemented by lidar data covering Ventura County that was acquired from the Ventura County Watershed Protection District (Airborne1, 2005). The lidar data was imported into ArcGIS to create a 1.5 m digital elevation model (DEM). Digital geomorphic maps comprising bare earth hillshade images and topographic slope maps were extracted from the DEM and used to reinterpret the spatial extent and increase the resolution of existing terrace maps (Rockwell, 1983; Rockwell, 1988) (Figs. 2 & 3). We extracted topographic profiles from the DEM and used these topographic profiles in combination with our digital geomorphic maps and field observations to confirm the presence of north-side-up tectonic scarps in Q4 and Q5 alluvial fans at the mouth of Orcutt Canyon (Fig. 3). Topographic profiles, geomorphic maps, and field observations were also employed to identify further alluvial surfaces offset by active faulting along the length of the proposed SSCF (Figs. 2 & 3).

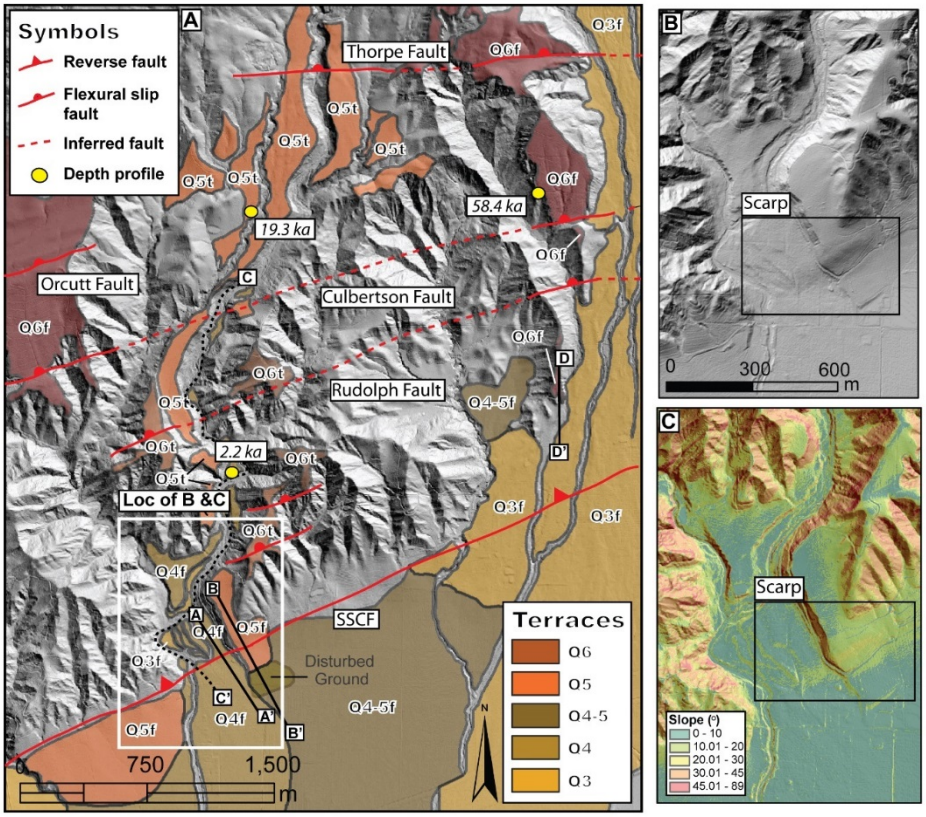

Figure 3 *Summary of active deformation at Orcutt Canyon. (A) Hillshade image with extent of mapped terraces and alluvial fans and the local surface trace of the Southern San Cayetano fault (SSCF) indicated with solid red line. Lines A-A' and B-B' show trace of topographic profiles through Q4 and Q5 surfaces at the mouth of Orcutt Canyon respectively. Topographic profiles are included in Figure 4. The trace of the modern-day stream used to calculate uplift of Q6 surfaces in Figure 4c is indicated by the dashed black line. (B) Hillshade map with 330° sun angle and 45° azimuth detailing scarp at the mouth of Orcutt Canyon. (C) Hillslope map with Orcutt Canyon scarp highlighted as pale green high angle slope against dark green low-angle slope detailing scarp at the mouth of Orcutt Canyon.*

Depth Profiles

We measured *in-situ*-produced cosmogenic ^{10}Be surface exposure ages using depth profiles (e.g. Anderson et al., 1996; DeVecchio et al., 2012). *In-situ* ^{10}Be is formed via the interaction of cosmic rays with minerals at the Earth's surface and the concentration of ^{10}Be decreases exponentially with

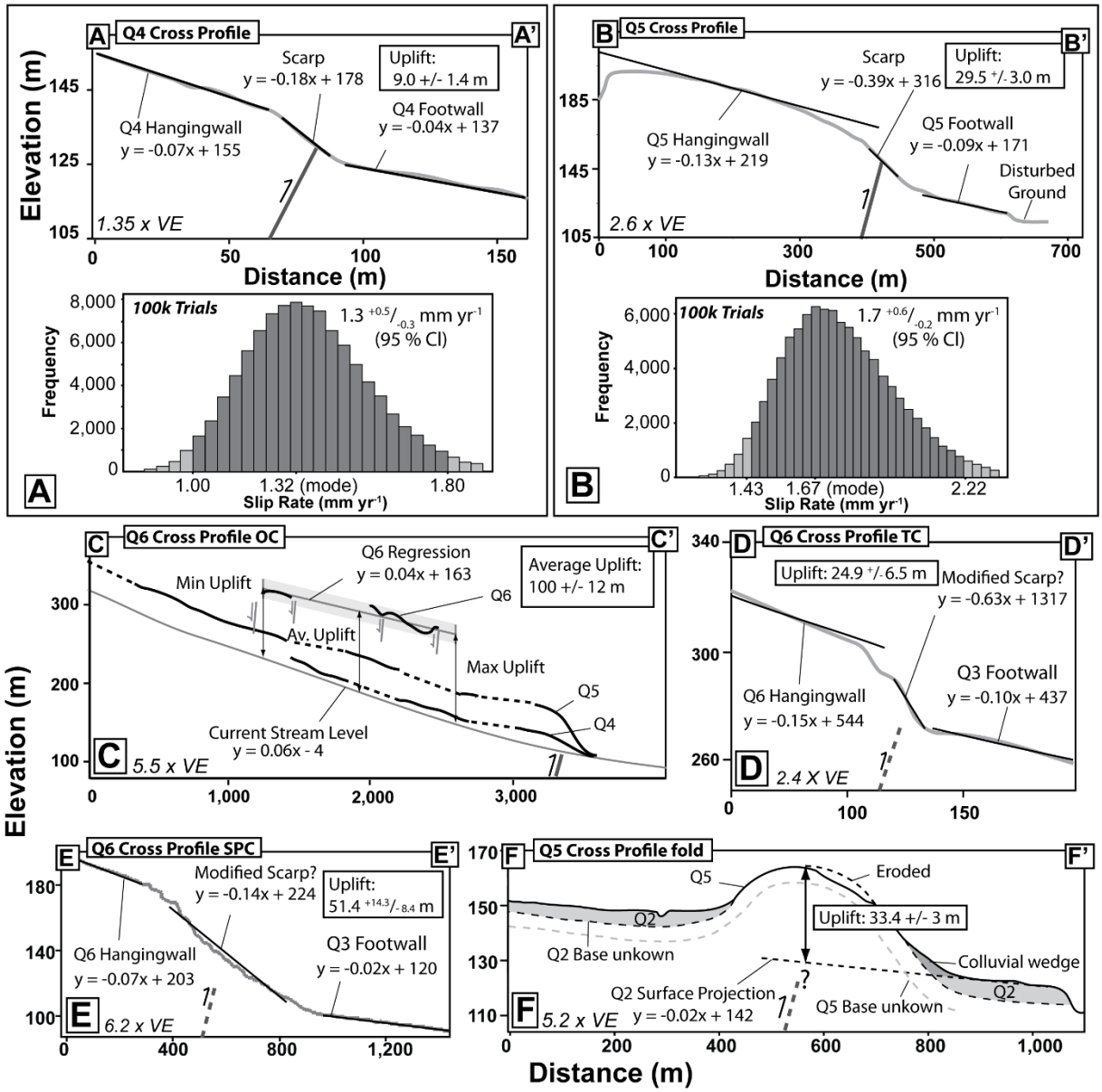

Figure 4 *Topographic profiles used to calculate displacement across the Southern San Cayetano fault (SSCF). Equations are linear regressions through geomorphic surfaces used in Monte Carlo simulations. A and B include topographic profiles A-A' and B-B' across the Q4 and Q5 surfaces at the mouth of Orcutt Canyon (lines of section in Figure 3) and frequency histograms of all slip rates output during Monte Carlo simulations. C includes section C-C' with a linear regression through the average elevation of the Q6 surface relative to the modern stream channel used to calculate average uplift and incision. The gray band either side of the regression denotes the vertical uncertainty. Bedding parallel flexural slip faults are indicated with pale gray lines. D and E are topographic profiles D-D' and E-E' through Q6 surfaces at Timber Canyon (D) and Santa Paula Creek (E) used to calculate minimum uplift for the Q6 surfaces relative to Q3 surfaces in the fault footwall. F is profile F-F', a topographic profile across the fold in the Santa Clara River Valley showing parameters used to calculate minimum uplift of the Q5 surface on the fold crest relative to the Q2 surface north and south of the fold. Lines of section for D-D' and C-C' are shown in Figure 3. Lines of section for E-E' and F-F' are shown in Figure 2. VE = Vertical exaggeration, OC = Orcutt Canyon, TC = Timber Canyon, SPC = Santa Paula Creek.*

depth. The surface ^{10}Be concentration represents the build-up of ^{10}Be since the time of surface abandonment and, if minimal erosion has occurred, the age of the surface. A depth profile accounts for substantial ^{10}Be acquired prior to deposition (inheritance) by estimating ^{10}Be concentration below the attenuation length of cosmic rays (Anderson et al., 1996). Depth profile locations were selected based on the quality and completeness of soil profile development. A complete soil profile is interpreted to indicate a stable surface that has not undergone significant erosion since time of

abandonment (Rockwell, 1983). We collected a total of 5 depth profile samples from alluvial fans with at Orcutt Canyon (Fig. 3) and Bear Canyon (Fig. 2a). Further samples for depth profiles were collected from an alluvial fill terrace at Orcutt Canyon (Fig. 3), the top surface of a folded Q5 alluvial fan in the Santa Clara River Valley (Fig. 2b), and an uplifted Q6 alluvial fan at neighboring Timber Canyon (Fig. 3).

Subsurface data

An approximately north-south oriented well-correlation section through Orcutt Canyon includes subsurface data for five wells down to ~3 km (Hopps et al., 1992). We reinterpreted well-log, lithological, and structural data contained in the correlation section to identify subsurface evidence for faulting at Orcutt Canyon. Additionally, two geotechnical reports encompassing trenching and/or shallow boreholes provide subsurface data along the western section of the range front and at Timber Canyon (Earth Consultants Earth Consultants International, 2015; Earth Systems Southern California, 2013).

Displacement rate calculations

Rates were calculated using Monte Carlo simulations by dividing either the total fault slip, fault throw, or uplift at each location by our new cosmogenic exposure ages. We assumed a fault dip at the surface of 50–90° and modeled uncertainties accordingly from the Monte Carlo simulation results.

RESULTS

Scarps

Bare earth hillshade imagery, topographic slope maps, topographic profiles, and field investigations confirm the presence of a north-side-up tectonic scarp in alluvial fans at the mouth of Orcutt Canyon (Figs. 3, 4a, & 4b). The scarp warps alluvial fans for ~420 m parallel to the trend of the range front and the surface trace of a range-front fault (Figs. 3, 4a, & 4b). Additionally, soil profiles exposed in road cuts perpendicular to the scarp have Q4 soil profile development both north and south of the scarp. We take the fact that the scarps follow the orientation of the potential range-front fault, along with the similarity of soil profiles north and south of the fault, to indicate a tectonic rather than erosional origin for the scarp.

^{10}Be terrace geochronology

Our new surface cosmogenic exposure-age determinations generally fall within the range of published soil age estimates, but with improved precision (DeVecchio et al., 2012; Rockwell, 1983) (Fig. 6). Our ages for both Q5 surfaces of 19.3 $^{+}/_{-}$ 2.7 ka (all ages are Bayesian most probable value with 2σ uncertainties throughout) for the Q5 terrace at Orcutt Canyon (Fig. 6) and 17.1 $^{+3.5}/_{-2.5}$ ka for the folded Q5 fan in the Santa Clara River Valley (Fig. 6) show good agreement, and overlap with the existing age for Q5 deposits within the Ventura basin (15-30 ka) (Rockwell, 1983). We revise the original designation of the uplifted fan surface at Timber Canyon from Q7 (160–200 ka) to Q6 (38–92 ka) (Rockwell, 1983). Revision is based on reevaluation of the soil profile in the field, the close match of the existing $Q6_b$ age of 54 ±10 ka (Rockwell, 1983) to our new cosmogenic numerical age (58.4 $^{+12.7}/_{-9.0}$ ka), and the similar value of tilt between a Q6 surface at Orcutt Canyon and the uplifted fan surface at Timber Canyon. However, it is possible the Q6 fan surface we dated at Timber Canyon may include remnants of Q7 soils in places, as described in Rockwell (1983). We discounted our age of 2.2 $^{+1.4}/_{-1.2}$ ka for the Q4 alluvial fill terrace at Orcutt Canyon. We suspect that a gravel channel in the top 1.5 m of the soil profile is a local, anomalously-young deposit and not representative of the age of the Q4 terrace we sampled. Consequently, we use our age of the Q4 fan at Bear Canyon of 7.3 $^{+1.8}/_{-1.7}$ ka (Fig. 2a) for our slip rate calculations at Orcutt Canyon.

Fault Geometry

Various datasets provide evidence for a north-dipping fault at Orcutt Canyon with 50–90° dip from the surface to ~100 m depth, below which the fault dip decreases to ~20° (Fig. 5). We employ a fault dip of 50–90° in our slip rate calculations and do not use the proposed subsurface dip of 20° because our displacement rates are calculated from surface offsets. On the well-correlation section through Orcutt Canyon, we note an abrupt change in dips that occurs at progressively shallower depths southwards for wells in the footwall of the San Cayetano fault (Hopps et al., 1992) (Fig. 5). The change in dips correlates to a fault with a shallow (~20°) north dip in the subsurface, with ~100 m of stratigraphic offset (Fig. 5). However, when projected to the surface, a fault with 20° north-dip that passes through the sections of variable dips observed in subsurface well-log data would steepen in dip in the upper ~100 m if it intersects with our preferred fault surface trace (Fig. 5). Fault evidence from borehole logs contained in a geotechnical report along the western section of the range front suggests a north-side-up sense of movement on three steeply-dipping northwest-southeast zones of faulting, with the majority of faults recording dips between 70–90° (Earth Systems Southern California, 2013). Additionally, we suggest the linear nature of the range front (Fig. 2) is indicative of a steep fault dip at the surface (assuming the location of the range front is fault controlled) and analysis of the intersection of the fault trace with the scarps suggests a range of apparent dips at the surface between 51–64°.

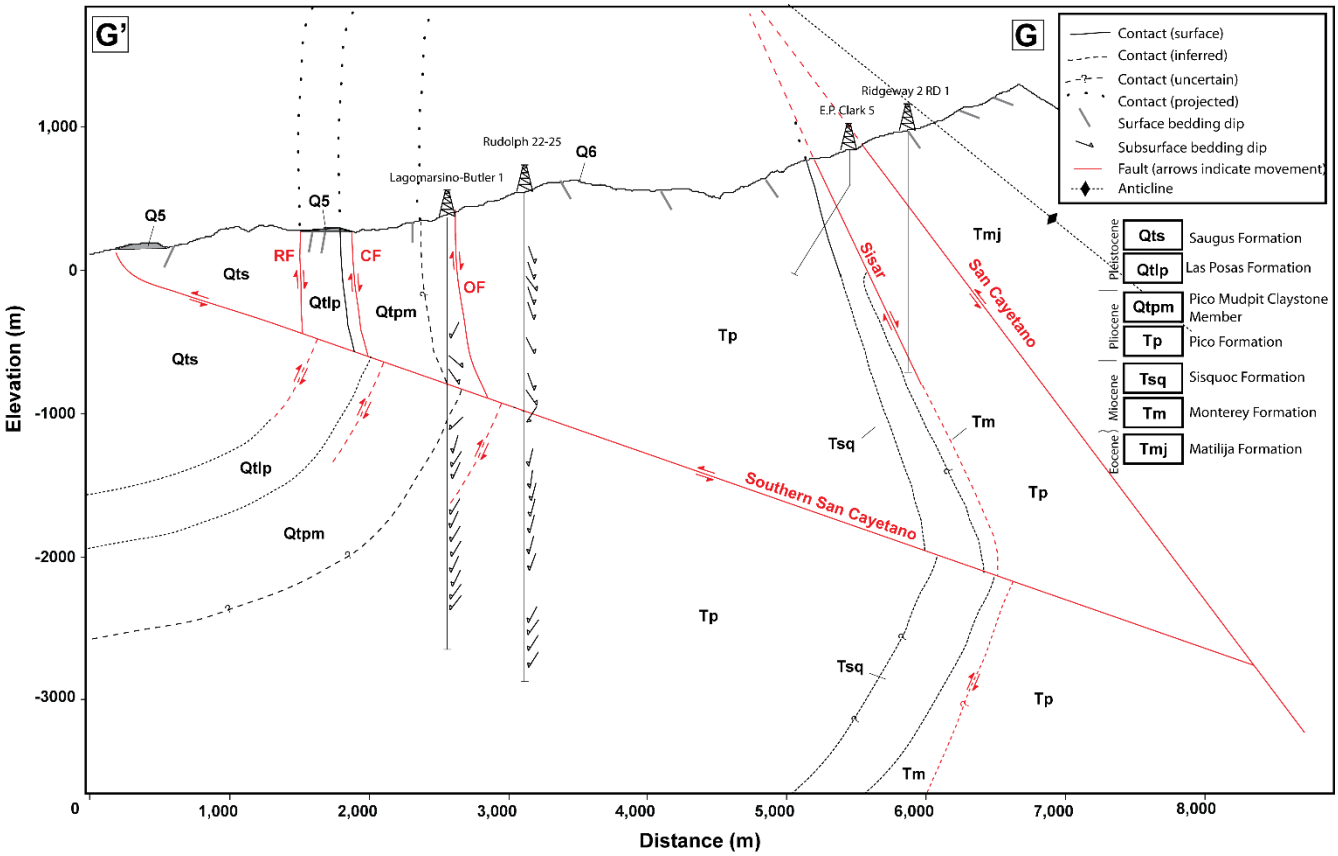

Figure 5 *Cross section G-G' showing our interpretation for the subsurface geometry for the Southern San Cayetano fault at Orcutt Canyon (after Hopps et al, 1992). Line of section is indicated in Figure 2. Surface dips and geology are from Dibblee (1990a). Well data is taken from Hopps et al (1992).*

This final report is based on work described in full within a recent paper published in *Earth and Planetary Science Letters* https://doi.org/10.1016/j.epsl.2018.10.003

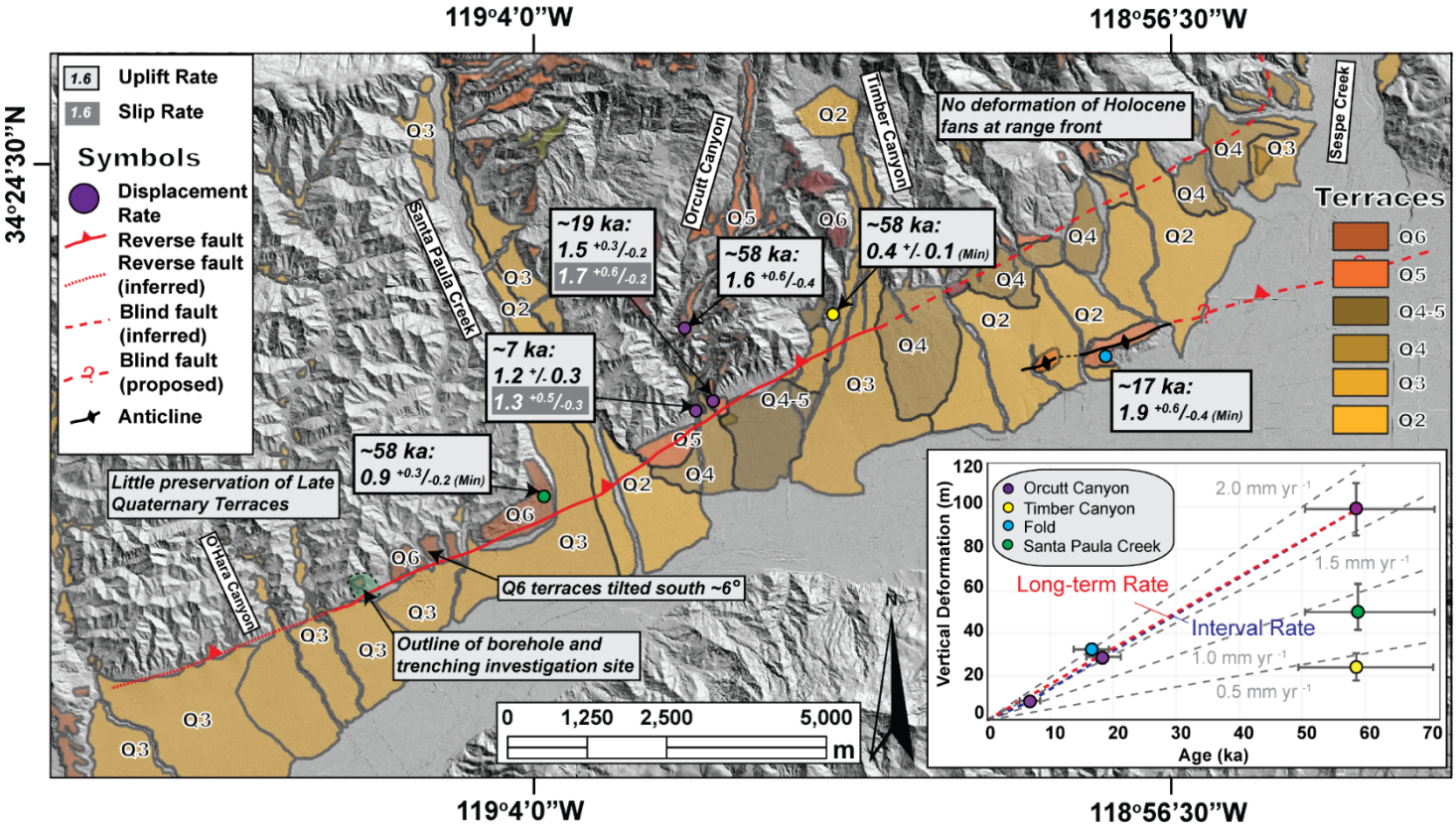

Figure 6 *Summary of spatial and temporal variations in slip rates and uplift rates for the Southern San Cayetano fault. Location of rate is indicated by colored circles (purple = Orcutt Canyon, yellow = Timber Canyon, green = Santa Paula Creek, and blue = Santa Clara River Valley). Vertical deformation (fault throw or uplift) is denoted using black text on a white background and fault slip rates are white text on gray background. Inset graph shows vertical deformation against surface age. Colored circles are uplift amounts with colors corresponding to the location of the rate on the map. Error bars are uncertainty in amount of vertical deformation (vertical error bars) or age (horizontal error bars) derived from Monte Carlo simulations. Deformation rates of 2.0, 1.5, 1.0, & 0.5 mm yr^{-1} are indicated with gray dashed lines. The red dashed line is the long-term uplift rate and interval rates are denoted by the blue dashed lines.*

Displacement rates

Within the resolution of our data, our results indicate that long-term average fault activity (fault uplift, throw, or slip) at Orcutt Canyon has remained relatively constant for the last ~58 ka (Fig. 6). Uplift amounts at Orcutt Canyon decrease with decreasing surface age, with 9.0 ± 1.4 m fault throw across the youngest Q4 scarp at the mouth of Orcutt Canyon and 99.7 ± 12.4 m average uplift of the oldest Q6 strath terrace relative to the modern-day stream level (Fig. 4). All uplift or fault throw rates at Orcutt Canyon overlap within uncertainties, with a maximum value of 1.7 $^{+0.7}/_{-0.4}$ mm yr^{-1} for the interval ~19–7 ka (deformation rates are mode and 95% confidence interval throughout) and a minimum value of 1.2 $^{+}/_{-}$ 0.3 mm yr^{-1} since ~7 ka (Fig. 6).

Fault slip rates also reflect a relatively constant rate of activity. The average fault slip rate from ~19 ka to the present day is 1.7 $^{+0.6}/_{-0.2}$ mm yr^{-1} and from ~7 ka to the present day the average slip rate is 1.3 $^{+0.5}/_{-0.3}$ mm yr^{-1}. The interval fault slip rate between ~19 ka and ~7 ka is 1.9 $^{+1.0}/_{-0.5}$ mm yr^{-1} (Fig. 6)

This final report is based on work described in full within a recent paper published in *Earth and Planetary Science Letters* **https://doi.org/10.1016/j.epsl.2018.10.003**

INTELLECTUAL MERIT

This project directly addresses the following SCEC5 Basic Questions of Earthquake Science: Question 1 (Q1) by refining slip-rates on a recently identified structure within the southern California fault system (**Priority 1.a**), Q3 by refining the geometry of active faults (**P3.a**), and Q5 by providing geologic constraints on large multi-fault ruptures (**P5.b**). Our work has also contributed to the Earthquake Geology Disciplinary Committee by 1) assisting in the quantification of along-strike variations in strain localization, specifically as it applies to multi-fault ruptures on major reverse faults in the WTR and 2) utilizing the Geochronology Infrastructure. It also directly contributes to the following Interdisciplinary Working Groups: Stress and Deformation Over Time (SDOT) and SCEC Community Models (SCM) by providing information on geologic fault slip rates and subsurface fault geometry that can be used to evaluate 1) deformation and earthquake cycle models and 2) the Community Fault Model (CFM), respectively. It has importance to the USGS EHP programs (i.e. National Seismic Hazard Mapping Program) and WGCEP. Our work provides a "proof of concept" dataset that can be used as leverage to pursue additional funding from other sources, including NSF and USGS NEHRP.

BROADER IMPACTS

This work supported one Masters student project and was conducted by PI Rood in conjunction with a PhD student as part of a wider PhD project investigating the tectonic geomorphology and seismic hazards of the Ventura Basin. The work provided one Masters student and two PhD students with valuable experience in earthquake geology field work, and enabled one Masters student and one PhD student to learn the theory, laboratory procedures, and application of cosmogenic isotopes in Earth Sciences. The work resulted in the following publication:

> *A. Hughes, D.H. Rood, A.C. Whittaker, R.E. Bell, T.K. Rockwell, Y. Levy, K.M. Wilcken, L.B. Corbett, P.R. Bierman, D.E. DeVecchio, S.T. Marshall, L.D. Gurrola, C. Nicholson, Geomorphic evidence for the geometry and slip rate of a young, low-angle thrust fault: Implications for hazard assessment and fault interaction in complex tectonic environments, Earth and Planetary Science Letters, Volume 504, 2018, Pages 198-210, ISSN 0012-821X, https://doi.org/10.1016/j.epsl.2018.10.003.*

REFERENCES

Airborne1, 2005. Ventura Rivers LiDAR dataset, project number A05-VENT-002.

Anderson, R.S., Repka, J.L. and Dick, G.S., 1996. Explicit treatment of inheritance in dating depositional surfaces using in situ 10Be and 26Al. Geology, 24(1): 47-51.

DeVecchio, D.E., Heermance, R.V., Fuchs, M. and Owen, L.A., 2012. Climate-controlled landscape evolution in the Western Transverse Ranges, California: Insights from Quaternary geochronology of the Saugus Formation and strath terrace flights. Lithosphere, 4(2): 110-130.

Dibblee Jr, T., 1990a. Geologic map of the Santa Paula Peak quadrangle. Ventura County, California: Dibblee Geological Foundation map# DF-26, Santa Barbara, California, scale, 1(24,000).

Dibblee Jr, T.W., 1990b. Geologic map of the Fillmore Quadrangle. Ventura County, California: Dibblee Geological Foundation map# DF-27, Santa Barbara, California, scale, 1(24,000).

Dolan, J.F., Bowman, D.D. and Sammis, C.G., 2007. Long-range and long-term fault interactions in Southern California. Geology, 35(9): 855-858.

Dolan, J.F. and Rockwell, T.K., 2001. Paleoseismologic evidence for a very large (M-w > 7), post-AD 1660 surface rupture on the eastern San Cayetano fault, Ventura County, California: Was this the elusive source of the damaging 21 December 1812 earthquake? Bulletin of the Seismological Society of America, 91(6): 1417-1432.

Dolan, J.F., Sieh, K., Rockwell, T.K., Yeats, R.S., Shaw, J., Suppe, J., Huftile, G.J. and Gath, E.M., 1995. Prospects for Larger or More Frequent Earthquakes in the Los-Angeles Metropolitan Region. Science, 267(5195): 199-205.

Earth Consultants International, 2015. Fault trenching study of the Culbertson fault in the Timber Canyon area east of Santa Paula, Ventura County, California. Earth Consultants International, Inc.

Earth Systems Southern California, 2013. Geo-Technical Feasibility Report for tract 5475, Santa Paula.

Field, E.H., Biasi, G.P., Bird, P., Dawson, T.E., Felzer, K.R., Jackson, D.D., Johnson, K.M., Jordan, T.H., Madden, C. and Michael, A.J., 2015. Long-term time-dependent probabilities for the third Uniform California Earthquake Rupture Forecast (UCERF3). Bulletin of the Seismological Society of America, 105(2A): 511-543.

Hopps, T., E, Stark, H., E and Hindle, R., J, 1992. Subsurface geology of Ventura Basin, California, Ventura Basin Study Group Report, 45 pp. 17 structure contour maps and 84 structure panels comprising 21 cross sections. Rancho Energy Consultants, Inc, Santa Paula, California.

Hubbard, J., Shaw, J.H., Dolan, J., Pratt, T.L., McAuliffe, L. and Rockwell, T.K., 2014. Structure and Seismic Hazard of the Ventura Avenue Anticline and Ventura Fault, California: Prospect for Large, Multisegment Ruptures in the Western Transverse Ranges. Bulletin of the Seismological Society of America, 104(3): 1070-1087.

Jennings, C. and Bryant, W., 2010. Fault activity map of California: California Geological Survey Geologic Data Map No. 6.

Marshall, S.T., Funning, G.J. and Owen, S.E., 2013. Fault slip rates and interseismic deformation in the western Transverse Ranges, California. Journal of Geophysical Research: Solid Earth, 118(8): 4511-4534.

Nicholson, C., Plesch, A., Sorlien, C.C., Shaw, J.H. and Hauksson, E., 2015. The SCEC Community Fault Model Version 5.0: An Updated And Expanded 3D Fault Set For Southern California, Pacific Section AAPG Convention.

Rockwell, T., 1983. Soil chronology, geology, and neotectonics of the northcentral Ventura basin, California: University of California, Santa Barbara, unpublished Ph. D, dissertation.

Rockwell, T., 1988. Neotectonics of the San-Cayetano Fault, Transverse Ranges, California. Geological Society of America Bulletin, 100(4): 500-513.

Shaw, J.H. and Suppe, J., 1996. Earthquake hazards of active blind-thrust faults under the central Los Angeles basin, California. Journal of Geophysical Research: Solid Earth, 101(B4): 8623-8642.

Wright, T.L., 1991. Structural geology and tectonic evolution of the Los Angeles basin, California. Active Margin Basins, 52: 35-134.